Department of Urology[1]; Department of Gynecology[2]; The Affiliated Yantai Yuhuangding Hospital of Qingdao University, Yantai, China

LncRNA HULC promotes epithelial and smooth-muscle-like differentiation of adipose-derived stem cells by upregulation of BMP9

Yongwei Li[1,#], Zhengfei Shan[1,#], Bin Yang[2,#], Diandong Yang[1], Changping Men[1], Yuanshan Cui[1], Jitao Wu[1,*]

Received May 12, 2017, accepted June 21, 2017

**Corresponding author: Jitao Wu, Department of Urology, The Affiliated Yantai Yuhuangding Hospital of Qingdao University, No. 20, East Yuhuangding Road, Yantai 264000, China*
wujitao1566@126.com.
 # These authors contributed equally to this work

Pharmazie 73: 49–55 (2018) *doi: 10.1691/ph.2018.7634*

Aims: Adipose-derived stem cells (ADSCs), a source of mesenchymal stem cells, are able to differentiate into numerous cell lineages, including epithelial and smooth muscle cells. The use of ADSCs in tissue engineering technology has become the most promising therapeutic approach for urethral reconstruction. This study aimed to explore the effect of lncRNA highly upregulated in liver cancer (HULC) on the induction of ADSCs to differentiate into epithelial and smooth-muscle-like cells. *Methods:* ADSCs were isolated from a male dog, and the expression of HULC in ADSCs was overexpressed by transfection with HULC expressing vector lentivirus. The transfected ADSCs were then incubated with 5 μM ATRA or 2.5 ng/ml TGF-β1 and 5 ng/ml PDGF-BB for 21 days. The expression of epithelial differentiation and smooth-muscle-like differentiation markers were monitored. Besides, cross-regulation between HULC and BMP9 was detected in the differentiated epithelial cells and smooth-muscle-like cells. *Results:* HULC increased cell viability of ADSCs, but has no impact on ADSCs apoptosis. HULC promotes ADSCs to differentiate into epithelial and smooth-muscle-like cells, as evidenced by the increases in the expression of Uroplakin-II, AE1/AE3, α-SMA, SM-MHC, Calponin, and SM-22α. In addition, HULC could positively regulate BMP9, and BMP9 silence abolished HULC-promoted ADSC's differentiation. Furthermore, HULC activated Wnt/β-catenin pathway while deactivated Notch pathway. *Conclusion:* HULC was demonstrated to be a promoter during the epithelial and smooth-muscle-like differentiation of ADSCs via the BMP9/Wnt/β-catenin/Notch network. This study provides the first *in vitro* evidence that HULC-based therapy could be a valuable approach to promote urethral reconstruction.

1. Introduction

Reconstruction of the adult and pediatric male penile urethra has been one of the great surgical challenges for urologists, especially in cases of recurrent hypospadias and long urethral defects after trauma (Liu et al. 2017). The use of tissue engineering technology has become one of the most promising therapeutic approaches for urethral reconstruction. As a source of mesenchymal stem cells (MSCs), adipose-derived stem cells (ADSCs) are found in the stromal-vascular fraction (SVF) of fat tissue (Ong and Sugii 2013). These cells have some advantages over other sources of stem cells, most notably that a large number of cells can be easily and quickly isolated from adipose tissue (Ong and Sugii 2013; Tobita and Mizuno 2013). ADSCs isolated from the stromal vascular fraction of adipose tissue are able to differentiate into numerous cell lineages, including adipogenic, osteogenic, chondrogenic, myogenic, neurogenic (Zachar et al. 2011), epithelial (Baer et al. 2011; Brzoska et al. 2005), and smooth muscle cells (Aji et al. 2017; Zhao et al. 2016). However, the paucity of available information about the molecular pathways that govern the epithelial and smooth-muscle-like differentiation of ADSCs has hampered further development of ADSC-based cell therapies.

Long non-coding RNAs (lncRNA), abundantly transcribed by the mammalian genome, are one kind of endogenous RNA comprising a sequence larger than 200 nucleotides (Yang et al. 2017). Expression of lncRNA that have putative roles in cell differentiation has been identified in embryonic and adult stem cells (Dallagiovanna et al. 2017). For instance, lncRNA MEG3 inhibits adipogenesis and promotes osteogenesis of human ADSCs via regulating miR-140-5p (Li et al. 2017). Knockdown of lncRNA MIAT promotes osteogenic differentiation of human ADSCs (Jin et al. 2017). Highly upregulated in liver cancer (HULC), a novel lncRNA, has attracted widespread attention (Chen et al. 2017). HULC gene is located on chromosome 6p24.3 with approximately 500 nucleotides in length and contains two exons (Yu et al. 2017). Abnormal expression of HULC has been found associated with metastasis and prognosis of many cancers, such as colorectal cancer, osteosarcoma, and gastric cancer (Sun et al. 2016; Uzan et al. 2016; Yang et al. 2016). In addition, HULC has been reported as a key molecular in human embryonic stem cells differentiation (Gui et al. 2015), and in regulatory T cells differentiation (Zhao et al. 2015).

In the present study, we aimed to explore the functional impacts of HULC on the induction of ADSCs to differentiate into epithelial and smooth-muscle-like cells and the possible mechanism. Results showed that HULC promoted the differentiation of epithelial and smooth-muscle-like cells derived from ADSCs possibly via BMP9 signaling pathway. This study provided the first evidence that HULC could be a therapeutic target in future urethral reconstruction therapy.

2. Investigations and results

2.1. HULC increases cell viability of ADSCs

As shown in Fig. 1A, the ADSCs were 98.97% pure for CD29, 99.23% for CD90, and 97.92% for CD105. The contaminated population of ADSCs positive to CD45 was 0.82%. ADSCs were then infected with HULC expressing vector lentivirus (pGC-HULC) or a mock lentivirus (pGC). The transduction efficiency was veri-

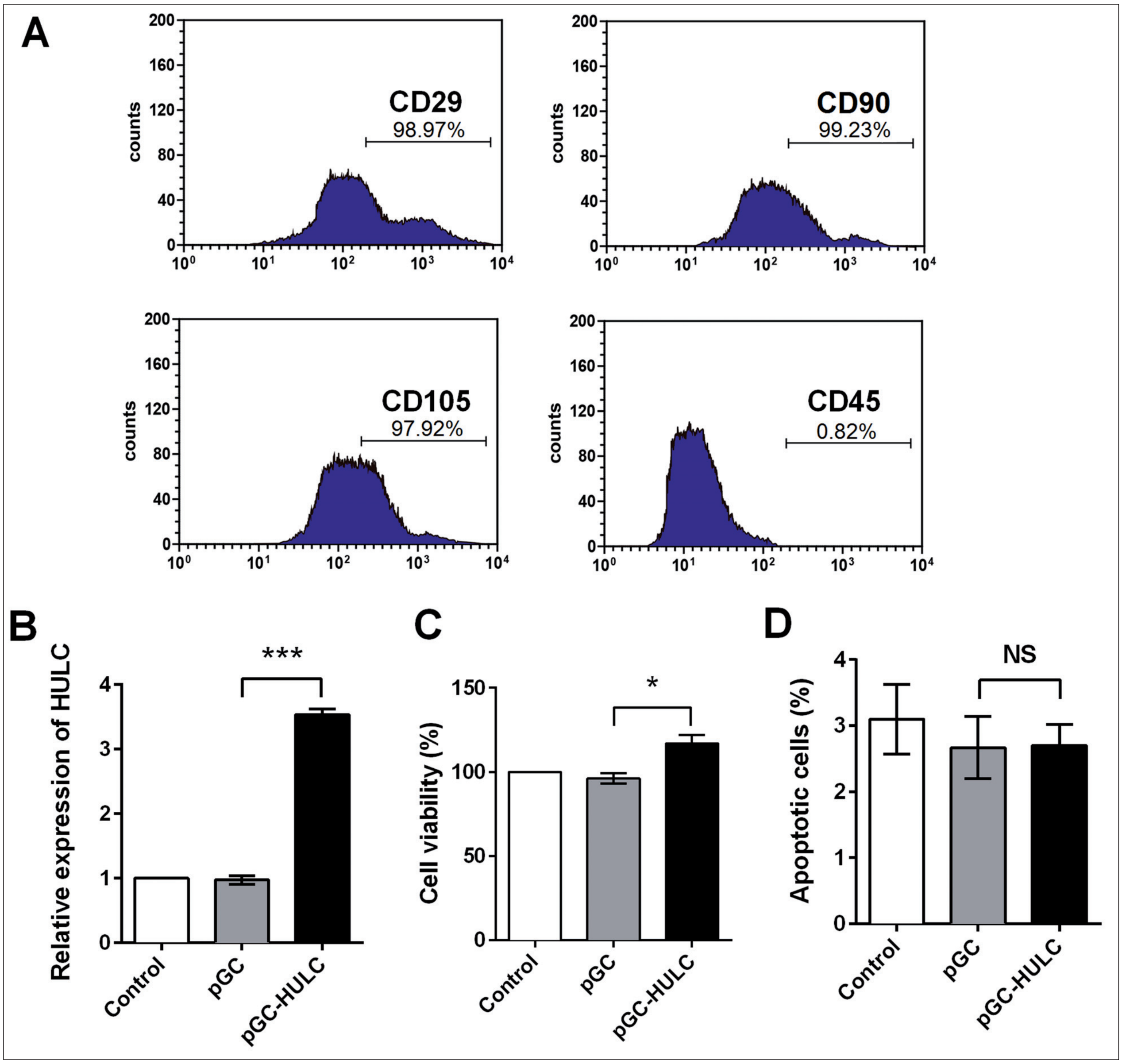

Fig. 1: HULC increases cell viability of ADSCs. (A) ADSCs identification was performed by flow cytometry analysis for CD29, CD90, CD105 and CD45. (B) The expression of HULC was measured by qRT-PCR after ADSCs were transfected with HULC expressing vector lentivirus (pGC-HULC) or its negative control (pGC). (C) Cell viability was detected by typan blue staining at 48 h post-transfection. (D) Apoptotic cells rate was detected by flow cytometer at 48 h post-transfection. Data represented as mean ± SD. n= 3 per group. NS, no significance; * $P < 0.05$; *** $P < 0.001$ compared to pGC group (ANOVA).

fied by qRT-PCR, and results showed that the expression level of HULC was significantly increased in pGC-HULC cells compared to pGC control ($P < 0.001$, Fig. 1B). Moreover, cell viability and apoptosis were respectively assessed to detect the impacts of HULC on the growth of ADSCs. As results shown in Fig. 1C, much higher cell viability was observed in pGC-HULC group than pGC group ($P < 0.05$); pGC-HULC resulting in a viability increase of 117±9%. However, no significant difference in apoptotic cells rate was found between the pGC-HULC group and the pGC group ($P > 0.05$, Fig. 1D).

2.2. *HULC promotes ADSCs to differentiate into epithelial cells*

After culturing the transfected ADSCs in ATRA for three weeks, the expression levels of Uroplakin-II and AE1/AE3 in cell were detected. As shown in Fig. 2A-2D, both the mRNA and protein levels of Uroplakin-II and AE1/AE3 were increased remarkably with prolonged epithelial induction. More importantly, Uroplakin-II and AE1/AE3 levels in pGC-HULC group were significantly higher than those in pGC group ($P < 0.05$, $P < 0.01$, or $P < 0.001$). These data suggested that HULC might play a role in the regulation of ADSC's epithelial differentiation.

2.3. *HULC promotes ADSCs to differentiate into smooth-muscle-like cells*

Meanwhile, the transfected ADSCs were cultured in TGF-β1 and PDGF-BB for three weeks, and the expression levels of α-SMA, SM-MHC, Calponin, and SM-22α in cells were detected, to reveal the impacts of HULC in ADSC's smooth-muscle-like differentiation. As shown in Fig. 3A-3H, both the mRNA and protein levels of these factors were all increased with prolonged smooth-muscle-like induction. Compared to pGC group, pGC-HULC group had much higher levels of α-SMA, SM-MHC, Calponin, and SM-22α ($P < 0.05$ or $P < 0.01$), indicating HULC

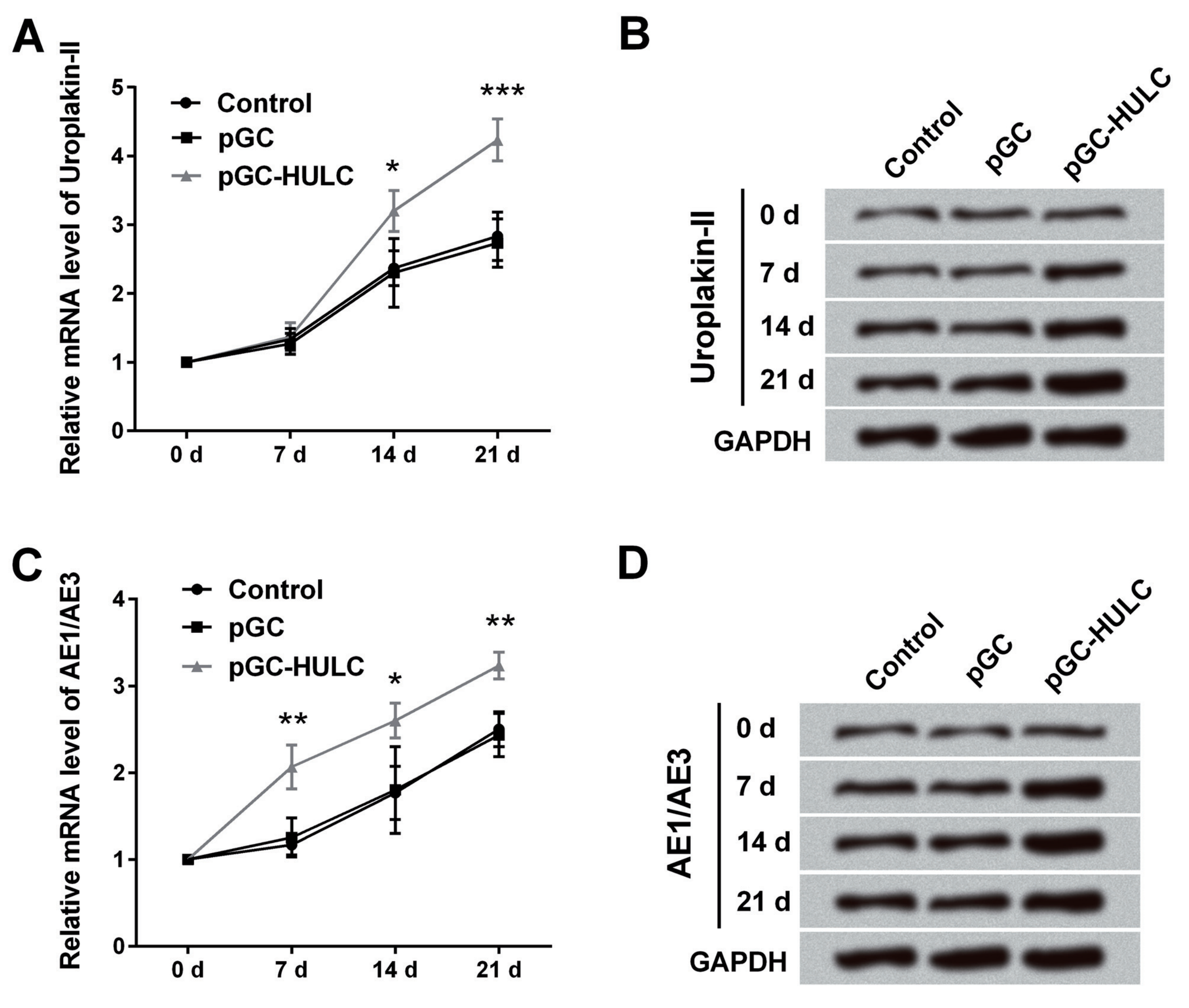

Fig. 2: HULC promotes ADSCs to differentiate into epithelial cells. ADSCs were transfected with HULC expressing vector lentivirus (pGC-HULC) or its negative control (pGC), and then exposed to ATRA for 21 days for induction of epithelial differentiation. The mRNA and protein expressions of (A-B) Uroplakin-II, and (C-D) AE1/AE3 were measured by qRT-PCR and western blot analysis at day 0, 7, 14, and 21. Data represented as mean ± SD. n= 3 per group. * $P < 0.05$; ** $P < 0.01$; *** $P < 0.001$ compared to pGC group (ANOVA).

might also play a role in the regulation of ADSC's smooth-muscle-like differentiation.

2.4. *BMP9 is involved in HULC promoted ADSC's differentiation*

Given that BMP9 plays a critical role in stem cell differentiation (Lamplot et al. 2013), it is possible that HULC promote ADSC's differentiation via BMP9 signaling pathway. Therefore, we detected cross-regulations between HULC and BMP9, and found that both the mRNA and protein levels of BMP9 were upregulated in HULC overexpressed ADSCs ($P < 0.01$, Fig. 4A-4B). These data implied a positive correlation between HULC and BMP9. Thereafter, we silenced BMP9 in ADSCs by transfection with the specific siRNA targeted BMP9, to explore the impact of BMP9 on HULC promoted ADSC's differentiation. As shown in Fig. 4C, the protein level of BMP9 was remarkably reduced after transfection with siBMP9. Of note, HULC induced increases in Uroplakin-II and AE1/AE3, as well as increases α-SMA, SM-MHC, Calponin, and SM-22α were all observably downregulated by BMP9 silencing (Fig. 4D). These data confirmed our hypothesis that BMP9 was involved in HULC promoted ADSC's differentiation.

2.5. *HULC activates Wnt/β-catenin pathway and deactivated Notch pathway*

It has been reported that BMP9-mediated stem cell differentiation via multiple signaling pathways, including Wnt/β-catenin, MAPK, HIF1α, Notch, etc (Lamplot et al. 2013). This study focused on the Wnt/β-catenin and Notch signaling pathways, and key components of these two pathways were detected by western blotting to investigate the capacity of HULC to regulate these factors. Results showed that, HULC elevated the expression of Wnt3a, Wnt5a and β-catenin, and these HULC-induced elevations were inhibited in the presence of siBMP9 (Fig. 5). However, Notch1, Notch2, and Notch3 were decreased by HULC, while these decreases induced by HULC were recovered by siBMP9. These data implied that HULC positively regulated BMP9, and thus activated the Wnt/β-catenin pathway, and deactivated the Notch pathway.

3. Discussion

Recently, several lncRNA have been reported as important regulators for the therapy or differentiation of stem cells (Dallagiovanna et al. 2017; Jin et al. 2017; Li et al. 2017). In this study, we demonstrated that, HULC increased cell viability of ADSCs, but has no impact on ADSCs apoptosis. HULC promotes ADSCs to differen-

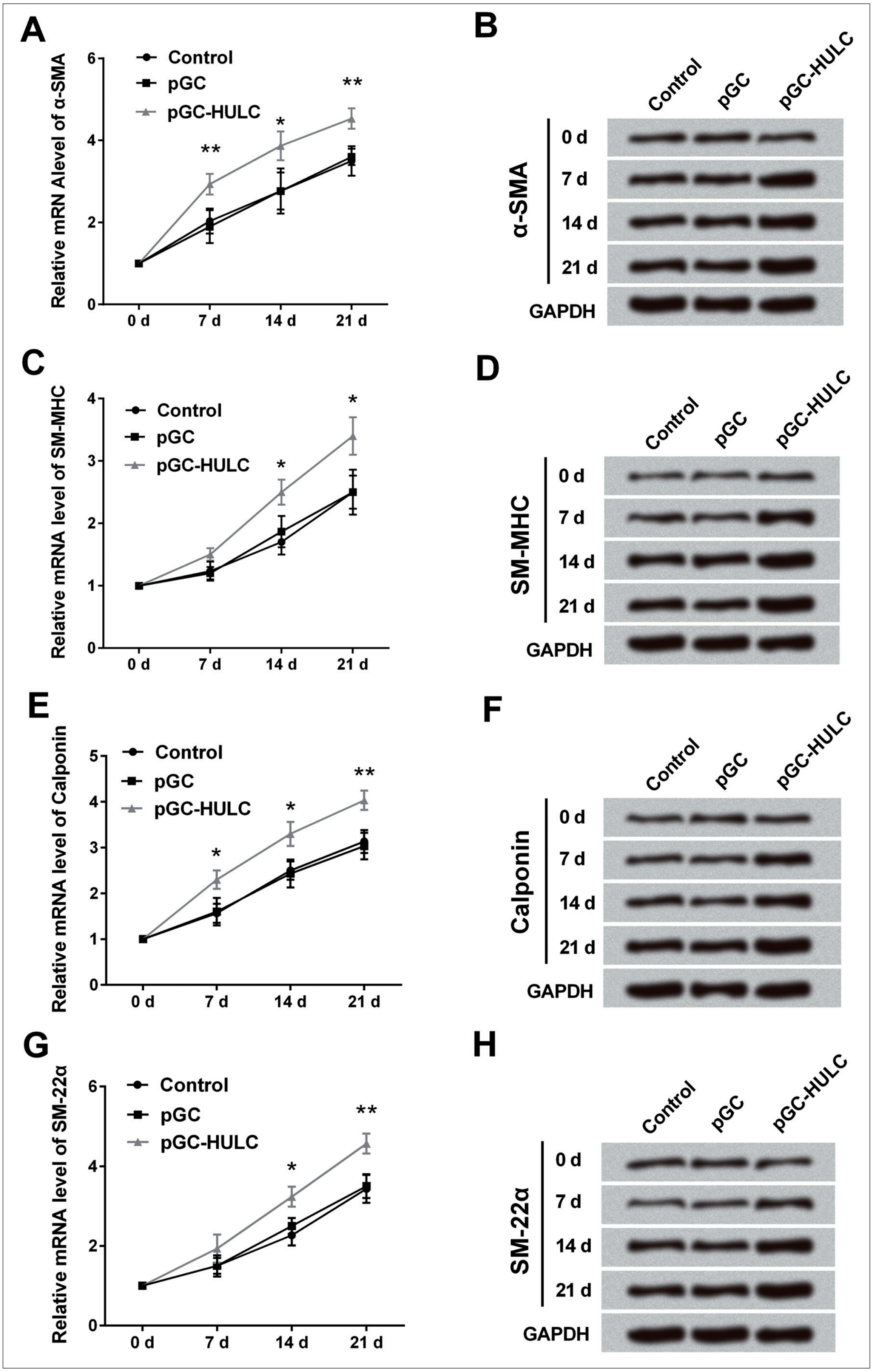

Fig. 3: HULC promotes ADSCs to differentiate into smooth-muscle-like cells. ADSCs were transfected with HULC expressing vector lentivirus (pGC-HULC) or its negative control (pGC), and then exposed to TGF-β1 and PDGF-BB for 21 days for induction of smooth-muscle-like differentiation. The mRNA and protein expressions of (A-B) α-SMA, (C-D) SM-MHC, (E-F) Calponin, and (G-H) SM-22α were measured by qRT-PCR and western blot analysis at day 0, 7, 14, and 21. Data represented as mean ± SD. n= 3 per group. * $P < 0.05$; ** $P < 0.01$ compared to pGC group (ANOVA).

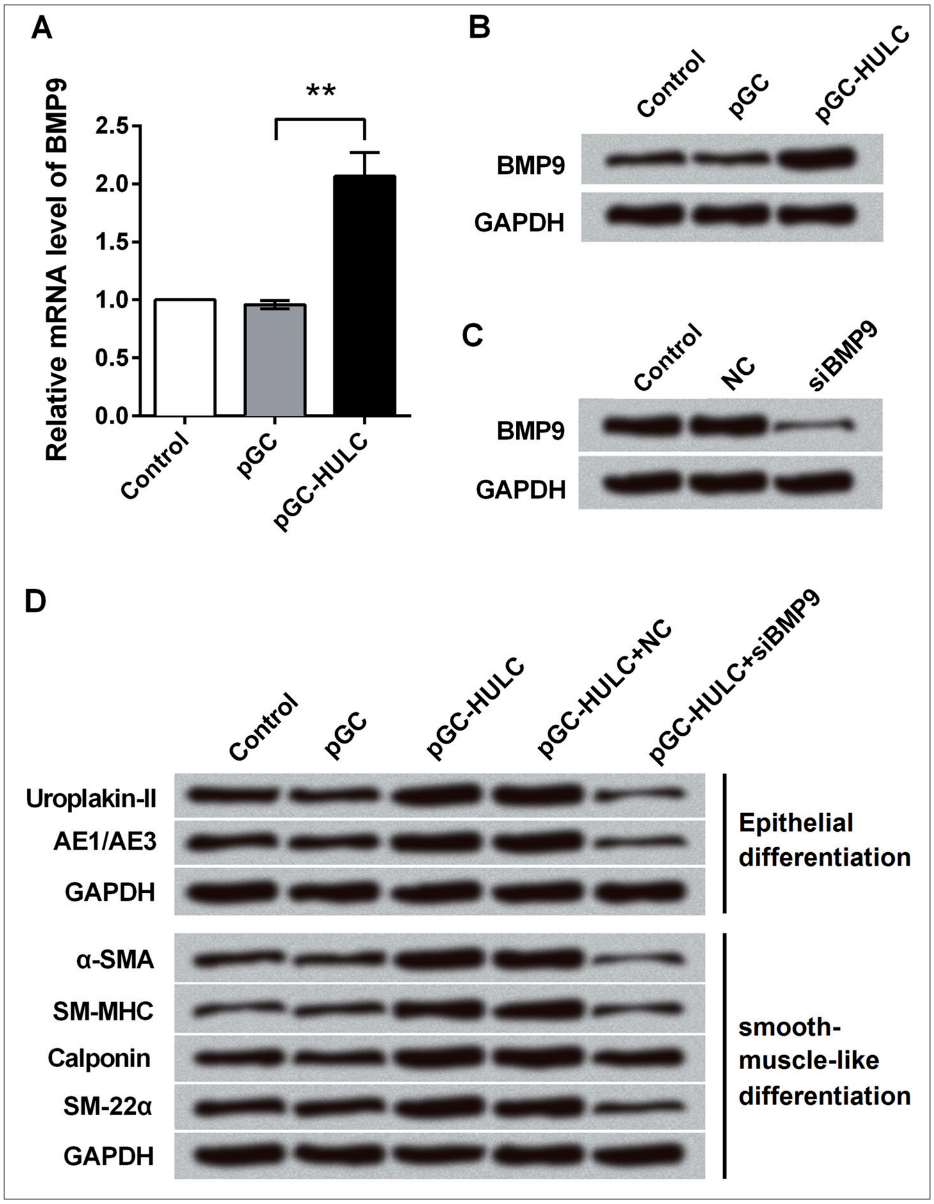

Fig. 4: BMP9 is involved in HULC promoted ADSC's differentiation. (A-B) The mRNA and protein levels of BMP9 were detected by qRT-PCR and western blotting after ADSCs were transfected with HULC expressing vector lentivirus (pGC-HULC) or its negative control (pGC). (C) The protein level of BMP9 were detected by western blotting after ADSCs were transfected with BMP9 targeted siRNA (siBMP9) or its negative control (NC). (D) ADSCs were co-transfected with pGC-HULC and siBMP9, and then exposed to ATRA, or TGF-β1 and PDGF-BB for 21 days for induction of epithelial or smooth-muscle-like differentiation. The protein expressions of Uroplakin-II, AE1/AE3, α-SMA, SM-MHC, Calponin, and SM-22α were measured by western blot analysis at day 21. Data represented as mean ± SD. n= 3 per group. ** $P < 0.01$ compared to pGC group (ANOVA).

tiate into epithelial and smooth-muscle-like cells, as evidenced by the increases in the expression of Uroplakin-II, AE1/AE3, α-SMA, SM-MHC, Calponin, and SM-22α. In addition, positive regulation between HULC and BMP9 was observed, and BMP9 silence abolished HULC-promoted ADSC's differentiation. Furthermore, HULC activated Wnt/β-catenin pathway while deactivated Notch pathway.

Autologous urothelial cells are considered to be the ideal seed cells for tissue-engineered urethra (Fossum and Nordenskjold 2010). However, they are difficult to obtain in quantity, since patients need to receive laparotomy for harvesting the autologous urothelial cells. On the other hand, ADSCs can be easily and abundantly obtained from "discarded" adipose tissue. In a recent report, ADSCs have demonstrated remarkable therapeutic potentials for the lower urinary tract, as ADSCs can differentiate into bladder smooth muscle and epithelial cells (Lin 2010). In another *in vivo* study, ADSCs can survive and integrate within rabbits' urethra walls, suggesting that autologous ADSCs transplantation is an alternative to intrinsic urethral regeneration (Almeida et al. 2010). This study was aimed to explore the strategies for improving ADSCs to differentiate into epithelial and smooth-muscle-like cells. We found that ectopic expression of HULC in ADSCs was conducive to ADSC's differentiation, implying that HULC could be a therapeutic target in future urethral reconstruction therapy.

Urothelial plaques consist of four major uroplakins (Ia, Ib, II, and III) that form two-dimensional crystals covering the apical surface

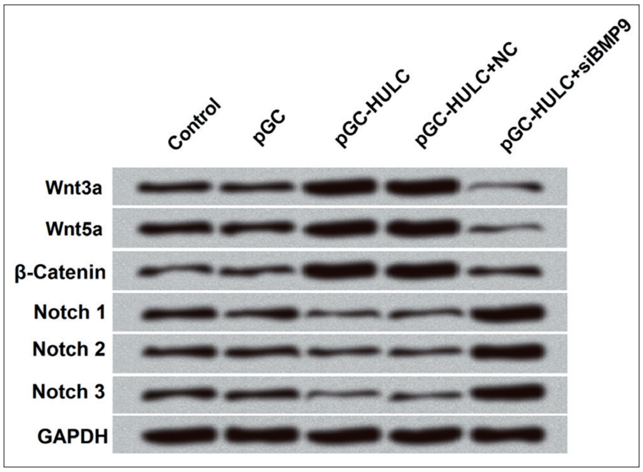

Fig. 5: HULC activates Wnt/β-catenin pathway and deactivates Notch pathway. ADSCs were co-transfected with HULC expressing vector lentivirus (pGC-HULC) and BMP9 targeted siRNA (siBMP9), and then the protein expressions of Wnt3a, Wnt5a, β-catenin, Nocth1, Notch2, and Notch3 were measured by western blot analysis.

of the urothelium (Deng et al. 2002). Nowadays, uroplakins have been widely used as markers of urothelial differentiation (Sun et al. 1999). Besides, uroplakins are markers specific for both transitional and stratified squamous epithelia and their carcinomas (Moll et al. 1995). AE1/AE3 is a mixture of two monoclonal antibodies, raised against human epidermal keratins (Woodcock-Mitchell et al. 1982). AE1 and AE3 recognize a wide spectrum of cytokeratins and their combinations are expressed during epithelial cell differentiation (Toniti et al. 2010). In this study, ADSCs transfected with HULC had much higher Uroplakin-II and AE1/AE3 levels than those of control cells, thereby suggesting that HULC may promote ADSCs to differentiate into epithelial cells.

It has been demonstrated that under the stimulation of TGF-β1 and PDGF-BB, MSCs could differentiate along the smooth muscle cell pathway characterized by the expression of specific contractile proteins, including α-SMA, SM-MHC, Calponin, and SM-22α (Antoon et al. 2012; Wang et al. 2010). α-SMA is an marker of smooth muscle, myofibroblasts and endothelial cells, thus its expression alone does not provide definitive evidence for an smooth muscle lineage (Wang et al. 2010). However, SM-22α, Calponin, and particularly SM-MHC are believed to be expressed in contractile smooth muscle cells only (Rensen et al. 2007). Calponin is a highly specific smooth muscle cell protein and an intermediated maturity marker, and SM-MHC as a protein related to smooth muscle cell maturity (Antoon et al. 2012). In this study, we demonstrated that HULC overexpressed ADSCs had high expression of α-SMA, SM-MHC, Calponin, and SM-22α upon synergistic induction with TGF-β1 and PDGF-BB *in vitro*. These findings suggested that HULC also could promote ADSCs to differentiate into smooth-muscle-like cells.

To further explore the mechanism(s) responsible for HULC promoted epithelial and smooth-muscle-like cell differentiation of ADSCs, we focused on the cross-regulation between HULC and BMP9. BMP9, also known as growth differentiation factor 2 or GDF-2, is a relatively poorly characterized member of the BMP family that was first isolated from fetal mouse liver cDNA libraries (Lamplot et al. 2013). Nowadays, BMP9 has been widely reported as a key regulator in promoting osteoblastic differentiation of MSCs (Beederman et al. 2013; Lamplot et al. 2013; Wang et al. 2017). However, to our knowledge, there is no report that BMP9 is implicated in the epithelial or smooth-muscle-like cells differentiation. However, BMP4, another member of the BMP family, has been reported as a costimulator of TGF-β1 to induce the differentiation of ADSCs to smooth muscle cells (Wang et al. 2010), and as a promoter in the differentiation of lung epithelial cells from mouse embryonic stem cells (Ninomiya et al. 2013). In this study, we found that BMP9 was positively regulated by HULC, and BMP9 silence abolished HULC-promoted epithelial and smooth-muscle-like cell differentiation from ADSCs. These findings provided the first evidence that HULC promoted epithelial and smooth-muscle-like differentiation of ADSCs by upregulation of BMP9.

Wnt/β-catenin and Notch are critical pathways important for self-renewal and specification of stem cells in multiple organs (Clevers et al. 2014; Yugawa et al. 2013). Immunohistochemistry data have shown differentiation of mouse intestinal epithelial cells under the targeted deletion Notch ligands (Nakata et al. 2017). Wnt/β-catenin pathway was activated during the differentiation of MSCs into alveolar epithelial cells (Gao et al. 2015). In addition, it has been found that Notch mediates Wnt and BMP signals in the early separation of smooth muscle progenitors and blood/endothelial common progenitors (Shin et al. 2009). In this study, we found that the Wnt/β-catenin pathway was activated by HULC while the Notch pathway was deactivated by HULC. Moreover, HULC-induced activation of Wnt/β-catenin and deactivation of Notch pathway were abolished by the addition of siBMP9. These findings indicated that HULC promoted epithelial and smooth-muscle-like differentiation of ADSCs via the BMP9/Wnt/β-catenin/Notch network. However, more work is required to confirm these hypotheses.

In conclusion, HULC was demonstrated to be a promoter during the epithelial and smooth-muscle-like differentiation of ADSCs via the BMP9/Wnt/β-catenin/Notch network. This study provides the first *in vitro* evidence that HULC-based therapy could be a valuable approach to promote urethral reconstruction.

4. Experimental

4.1. Dog ADSCs isolation and cell culture

ADSCs were isolated from a dog according to the method described by Alamoudi et al. (2014). A male dog (2 year old, weight 9.2 kg) having a systemically healthy condition was included in this study. All the animal experiments performed in this study were approved by the Animal Ethics Committee of The Affiliated Yantai Yuhuangding Hospital of Qingdao University and were conducted in accordance with the instruction of our institute. Under general anesthesia with isoflurane inhalation, adipose tissue was isolated from omentum and the inguinal fat pad of dog. Adipose tissues were washed twice with phosphate buffered solution (PBS) and then finely minced with scissors and digested with 0.075% collagenase II (Sigma-Aldrich, St Louis, MO, USA) for 1 h at 37 °C with gentle shaking. After the samples were centrifuged at 400 × *g* for 5 min at 4 °C, the cells were planted into tissue culture flasks in Dulbecco's modified Eagle's medium (DMEM, Gibco, Carlsbad, CA, USA) supplemented with 10% fetal bovine serum (FBS, Gibco). Cells were cultured at 37 °C in humidified atmosphere under 5% CO_2. After 48 h, the non-adherent cells were discarded by a PBS wash.

For ADSCs identification, 1 × 10^5 ADSCs at passage three were incubated with PE-conjugated anti-CD29, anti-CD45 or anti-CD90 and FITC-conjugated anti-CD105 (1:100 dilution, BD Biosciences, San Jose, CA) for 30 min at room temperature. The labeled cells were then washed twice with PBS and analyzed using a flow cytometer (BD FACSAriaTM III system; BD Pharmingen).

4.2. Lentiviral vectors construction and transfection

HULC expressing vector lentivirus pGC-FU-HULC-GFP was constructed by Genechem (Shanghai, China). The ADSCs infected with lentivirus pGC-FU-HULC-GFP were defied as pGC-HULC, and the ADSCs infected with mock lentivirus were defined as pGC, which were used as a negative control (NC). To achieve the optimal gene transfer, 8 μg/ml polybrene (Sigma-Aldrich) was used to assist the uptake of viral particles.

4.3. qRT-PCR

Total RNA was isolated from transfected ADSCs by using TRIzol reagent (Invitrogen) and treated with DNaseI (Promega). Reverse transcription was performed by using the Multiscribe RT kit (Applied Biosystems) and random hexamers or oligo(dT). The reverse transcription conditions were 10 min at 25 °C, 30 min at 48 °C, and a final step of 5 min at 95 °C. qRT-PCR was carried out by using TaqMan Power SYBR Green PCR Mix (Invitrogen), and amplification reactions were performed under the ABI PRISM 7500 Sequence Detection System (Applied Biosystems). Data were calculated by the $2^{-\Delta\Delta C}$ method (Livak and Schmittgen 2001). The internal control gene was GAPDH.

4.4. Cell viability assay

After the transfected ADSCs were incubated in fresh medium for 48 h, cell viability was detected by the using a Typan Blue Staining Cell Viability Assay Kit (Beyotime, Shanghai, China). In brief, 5 × 10^3 ADSCs were resuspended in 1 ml cell resuspension solution, and then 1 ml trypan blue solution was added. After the samples were incubated for 5 min at room temperature, cells were counted using a hemocytometer. Viability was calculated as % cell viability = living/total cells × 100%.

4.5. Apoptosis assay

Quantification of apoptosis was performed by using an Annexin V-FITC Apoptosis Detection Kit (Beyotime). Briefly, 1 × 10^5 transfected ADSCs were seeded in 6-well plates and allowed for incubation at 37 °C for 48 h. The cells were resuspended in 200 μL binding buffer, stained with 10 μL FITC-annexin V and 5 μL PI for 30 min in the dark at room temperature. Then 300 μL PBS was added, and cells were analyzed by the flow cytometer (BD FACSAriaTM III system) and BD CellQuest™ software version 5.1 (BD Biosciences).

4.6. Differentiation of ADSCs

The induction of epithelial differentiation was performed as previously described (Brzoska et al. 2005). ADSCs at passage 3 were incubated with ATRA (Sigma-Aldrich) at a final concentration of 5 μM. For cell culture, ATRA was dissolved in low glucose (1000 mg/l) DMEM substituted with 10% FBS. The medium was replaced every two days during a total incubation period of 21 days.

For smooth-muscle-like differentiation, ADSCs at passage 3 were incubated with 2.5 ng/ml TGF-β1 and 5 ng/ml PDGF-BB (both from Sigma-Aldrich), based on dosages used in prior study (Antoon et al. 2012). TGF-β1 and PDGF-BB were dissolved in low glucose (1000 mg/l) DMEM substituted with 10% FBS. The medium was replaced every two days during a total incubation period of 21 days.

4.7. *miRNAs transfection*

Small interfering RNA (siRNA) against BMP9 and control siRNA was synthesized by GenePharma (Shanghai, China). Cell transfections were conducted using Lipofectamine 3000 reagent (Invitrogen) following the manufacturer's protocol.

4.8. *Western blot analysis*

Cellular protein was extracted using RIPA lysis buffer (Beyotime, Shanghai, China). Quantitation of protein was conducted by using the BCA™ Protein Assay Kit (Pierce, Appleton, WI, USA). The whole-protein samples were resolved over 10 %-12 % sodium dodecyl sulfate polyacrylamide gel electrophoresis (SDS-PAGE) and transferred to a polyvinylidene fluoride membrane. Followed by blocking in 5 % skim milk for 1 h at room temperature, the membranes were incubated with primary antibodies: rabbit anti-Uroplakin-II (1:50 dilution, Catalog No.: 365527, US Biological, Swampscott, MA), mouse anti-AE1/AE3 (1:200 dilution, Catalog No.: sc-81714, Santa Cruz Biotechnology, Santa Cruz, CA), mouse anti-α-SMA (1:5000 dilution, Catalog No.: 40482, Signalway Antibody LLC), rabbit anti-SM-MHC (1:1000 dilution, Catalog No.: ab53219, Abcam, Cambridge, MA), rabbit anti-Calponin (1:1000 dilution, Catalog No.: ab46794, Abcam), rabbit anti-SM-22α (1:1000 dilution, Catalog No.: ab14106, Abcam), rabbit anti-BMP9 (1:1000 dilution, Catalog No.: ab35088, Abcam), rabbit anti-Wnt3a (1:1000 dilution, Catalog No.: ab28472, Abcam), rabbit anti-Wnt5a (1:1000 dilution, Catalog No.: ab174963, Abcam), rabbit anti-β-catenin (1:1000 dilution, Catalog No.: ab16051, Abcam), rabbit anti-Notch1 (1:1000 dilution, Catalog No.: ab52627, Abcam), rabbit anti-Notch2 (1:1000 dilution, Catalog No.: ab118824, Abcam), and rabbit anti-Notch3 (1:1000 dilution, Catalog No.: ab23426, Abcam), overnight at 4 °C. Mouse anti-GAPDH (1:1000 dilution, Catalog No.: ab8245, Abcam) was used as an internal control. The membranes were then incubated with the secondary anti-rabbit IgG (1:2000 dilution, ab191866, Abcam) and anti-mouse IgG (1:2000 dilution, ab193651, Abcam) for 1 h at room temperature. Blots were visualized by enhanced chemiluminescence (ECL) method.

4.9. *Statistical analysis*

All experiments were repeated three times. The results of multiple experiments are presented as the mean±standard derivations (SD). Statistical analyses were performed using Graphpad 6.0 statistical software (GraphPad Software Inc., San Diego, CA). The *P*-values were calculated using a one-way analysis of variance (ANOVA). A *P*-value of <0.05 was considered to indicate a statistically significant result.

Funding: This study was supported by the National Nature Science Foundation of China (No. 81500587; No. 81572835, No. 81700664), and by the Nature Science Foundation of Shandong Province (NO. ZR2016HP38).

Conflict of interest: None declared.

References

Aji K, Zhang Y, Aimaiti A, Wang Y, Rexiati M, Azhati B, Tusong H, Cui L, Wang C (2017) MicroRNA-145 regulates the differentiation of human adipose-derived stem cells to smooth muscle cells via targeting Kruppel-like factor 4. Mol Med Rep 15: 3787-3795.

Alamoudi NM, El Ashiry EA, Farsi NM, El Derwi DA, Atta HM (2014) Treatment of oral ulcers in dogs using adipose tissue-derived mesenchymal stem cells. J Clin Pediatr Dent 38: 215-222.

Almeida FG, Nobre YT, Leite KR, Bruschini H (2010) Autologous transplantation of adult adipose derived stem cells into rabbit urethral wall. Int Urogynecol J 21: 743-748.

Antoon R, Yeger H, Loai Y, Islam S, Farhat WA (2012) Impact of bladder-derived acellular matrix, growth factors, and extracellular matrix constituents on the survival and multipotency of marrow-derived mesenchymal stem cells. J Biomed Mat Res Part A 100: 72-83.

Baer PC, Brzoska M, Geiger H (2011) Epithelial differentiation of human adipose-derived stem cells. Methods Mol Biol 702: 289-298.

Beederman M, Lamplot JD, Nan G, Wang J, Liu X, Yin L, Li R, Shui W, Zhang H, Kim SH, Zhang W, Zhang J, Kong Y, Denduluri S, Rogers MR, Pratt A, Haydon RC, Luu HH, Angeles J, Shi LL, He TC (2013) BMP signaling in mesenchymal stem cell differentiation and bone formation. J Biomed Sci Engin 6: 32-52.

Brzoska M, Geiger H, Gauer S, Baer P (2005) Epithelial differentiation of human adipose tissue-derived adult stem cells. Biochem Biophys Res Commun 330: 142-150.

Chen X, Lin J, Liu Y, Peng J, Cao Y, Su Z, Wang T, Cheng J, Hu D (2017) AlncRNA HULC as an effective biomarker for surveillance of the outcome of cancer: A meta-analysis. PLoS One 12: e0171210.

Clevers H, Loh KM, Nusse R (2014) Stem cell signaling. An integral program for tissue renewal and regeneration: Wnt signaling and stem cell control. Science 346: 1248012.

Dallagiovanna B, Pereira IT, Origa-Alves AC, Shigunov P, Naya H, Spangenberg L (2017) lncRNAs are associated with polysomes during adipose-derived stem cell differentiation. Gene 610: 103-111.

Deng FM, Liang FX, Tu L, Resing KA, Hu P, Supino M, Hu CC, Zhou G, Ding M, Kreibich G, Sun TT (2002) Uroplakin IIIb, a urothelial differentiation marker, dimerizes with uroplakin Ib as an early step of urothelial plaque assembly. J Cell Biol 159: 685-694.

Fossum M, Nordenskjold A (2010) Tissue-engineered transplants for the treatment of severe hypospadias. Horm Res Paediatr 73: 148-152.

Gao P, Yang J, Gao X, Xu D, Niu D, Li J, Wen Q (2015) Salvianolic acid B improves bone marrow-derived mesenchymal stem cell differentiation into alveolar epithelial cells type I via Wnt signaling. Mol Med Rep 12: 1971-1976.

Gui X, Li H, Li T, Pu H, Lu D (2015) Long noncoding RNA CUDR regulates HULC and beta-catenin to govern human liver stem cell malignant differentiation. Mol The 23: 1843-1853.

Jin C, Zheng Y, Huang Y, Liu Y, Jia L, Zhou Y (2017) Long non-coding RNA MIAT knockdown promotes osteogenic differentiation of human adipose-derived stem cells. Cell Biol Int 41: 33-41.

Lamplot JD, Qin J, Nan G, Wang J, Liu X, Yin L, Tomal J, Li R, Shui W, Zhang H, Kim SH, Zhang W, Zhang J, Kong Y, Denduluri S, Rogers MR, Pratt A, Haydon RC, Luu HH, Angeles J, Shi LL, He TC (2013) BMP9 signaling in stem cell differentiation and osteogenesis. Am J Stem Cells 2: 1-21.

Li Z, Jin C, Chen S, Zheng Y, Huang Y, Jia L, Ge W, Zhou Y (2017) Long non-coding RNA MEG3 inhibits adipogenesis and promotes osteogenesis of human adipose-derived mesenchymal stem cells via miR-140-5p. Mol Cell Biochem doi: 10.1007/s11010-017-3015-z.

Lin CS (2010) Advances in stem cell therapy for the lower urinary tract. World J Stem Cells 2: 1-4.

Liu Y, Ma W, Liu B, Wang Y, Chu J, Xiong G, Shen L, Long C, Lin T, He D, Butnaru D, Alexey L, Zhang Y, Zhang D, Wei G (2017) Urethral reconstruction with autologous urine-derived stem cells seeded in three-dimensional porous small intestinal submucosa in a rabbit model. Stem Cell Res Ther 8: 63.

Livak KJ, Schmittgen TD (2001) Analysis of relative gene expression data using real-time quantitative PCR and the 2(-Delta Delta C(T)) Method. Methods 25: 402-408.

Moll R, Wu XR, Lin JH, Sun TT (1995) Uroplakins, specific membrane proteins of urothelial umbrella cells, as histological markers of metastatic transitional cell carcinomas. Am J Pathol 147: 1383-1397.

Nakata T, Shimizu H, Nagata S, Ito G, Fujii S, Suzuki K, Kawamoto A, Ishibashi F, Kuno R, Anzai S, Murano T, Mizutani T, Oshima S, Tsuchiya K, Nakamura T, Hozumi K, Watanabe M, Okamoto R (2017) Data showing proliferation and differentiation of intestinal epithelial cells under targeted depletion of Notch ligands in mouse intestine. Data in Brief 10: 551-556.

Ninomiya N, Michiue T, Asashima M, Kurisaki A (2013) BMP signaling regulates the differentiation of mouse embryonic stem cells into lung epithelial cell lineages. In vitro Cell Dev Biol Anim 49: 230-237.

Ong WK, Sugii S (2013) Adipose-derived stem cells: fatty potentials for therapy. Int J Biochem Cell Biol 45: 1083-1086.

Rensen SS, Doevendans PA, van Eys GJ (2007) Regulation and characteristics of vascular smooth muscle cell phenotypic diversity. Netherlands Heart J 15: 100-108.

Shin M, Nagai H, Sheng G (2009) Notch mediates Wnt and BMP signals in the early separation of smooth muscle progenitors and blood/endothelial common progenitors. Development (Cambridge, England) 136: 595-603.

Sun TT, Liang FX, Wu XR (1999) Uroplakins as Markers of Urothelial Differentiation. Adv Exp Med Biol 462: 7-18; discussion 103-114.

Sun W, Yang Y, Xu C, Xie Y, Guo J (2016) Roles of long noncoding RNAs in gastric cancer and their clinical applications. J Cancer Res Clin Oncol 142: 2231-2237.

Tobita M, Mizuno H (2013) Adipose-derived stem cells and periodontal tissue engineering. Int J Oral Maxillofac Implants 28: e487-493.

Toniti P, Sirivisoot S, Jandee P, Srimontri P, Puchadapirom P, Doungchawee G, Kasorndorkbua C (2010) AE1/AE3, vimentin and p63 immunolocalization in canine mammary gland tumours: roles in differentiation between luminal epithelial and myoepithelial lineages. Asian Pac J Cancer Prev 11: 227-230.

Uzan VR, Lengert A, Boldrini E, Penna V, Scapulatempo-Neto C, Scrideli CA, Filho AP, Cavalcante CE, de Oliveira CZ, Lopes LF, Vidal DO (2016) High expression of HULC is associated with poor prognosis in osteosarcoma patients. PLoS One 11: e0156774.

Wang C, Yin S, Cen L, Liu Q, Liu W, Cao Y, Cui L (2010) Differentiation of adipose-derived stem cells into contractile smooth muscle cells induced by transforming growth factor-beta1 and bone morphogenetic protein-4. Tissue Engin A 16: 1201-1213.

Wang F, Jiang Y, Huang X, Liu Q, Zhang Y, Luo W, Zhang F, Zhou P, Lin J, Zhang H (2017) Pro-inflammatory cytokine TNF-alpha attenuates BMP9-induced osteo/odontoblastic differentiation of the stem cells of dental apical papilla (SCAPs). Cell Physiol Biochem 41: 1725-1735.

Woodcock-Mitchell J, Eichner R, Nelson WG, Sun TT (1982) Immunolocalization of keratin polypeptides in human epidermis using monoclonal antibodies. J Cell Biol 95: 580-588.

Yang XJ, Huang CQ, Peng CW, Hou JX, Liu JY (2016) Long noncoding RNA HULC promotes colorectal carcinoma progression through epigenetically repressing NKD2 expression. Gene 592: 172-178.

Yang Y, Wang S, Li T (2017) Altered long non-coding RNAs predict worse outcome in osteosarcoma patients: evidence from a meta-analysis. Oncotarget 8: 35234-35243.

Yu X, Zheng H, Chan MT, Wu WK (2017) HULC: an oncogenic long non-coding RNA in human cancer. J Cell Mol Med 21: 410-417.

Yugawa T, Nishino K, Ohno S, Nakahara T, Fujita M, Goshima N, Umezawa A, Kiyono T (2013) Noncanonical NOTCH signaling limits self-renewal of human epithelial and induced pluripotent stem cells through ROCK activation. Mol Cell Biol 33: 4434-4447.

Zachar V, Rasmussen JG, Fink T (2011) Isolation and growth of adipose tissue-derived stem cells. Methods Mol Biol (Clifton, N.J.) 698: 37-49.

Zhao J, Fan Y, Wang K, Ni X, Gu J, Lu H, Lu Y, Lu L, Dai X, Wang X (2015) LncRNA HULC affects the differentiation of Treg in HBV-related liver cirrhosis. Int Immunopharmacol 28: 901-905.

Zhao Z, Yu H, Fan C, Kong Q, Liu D, Meng L (2016) Differentiate into urothelium and smooth muscle cells from adipose tissue-derived stem cells for ureter reconstruction in a rabbit model. Am J Translat Res 8: 3757-3768.